ChemPubSoc Europe

DOI: 10.1002/cssc.201601220

CHEMSUSCHEM Full Papers

Integrating Reverse-Electrodialysis Stacks with Flow Batteries for Improved Energy Recovery from Salinity Gradients and Energy Storage

Xiuping Zhu,*[a, b] Taeyoung Kim,[a] Mohammad Rahimi,[c] Christopher A. Gorski,[a] and Bruce E. Logan[a]

Salinity gradient energy can be directly converted into electrical power by using reverse electrodialysis (RED) and other technologies, but reported power densities have been too low for practical applications. Herein, the RED stack performance was improved by using 2,6-dihydroxyanthraquinone and ferrocyanide as redox couples. These electrolytes were then used in a flow battery to produce an integrated RED stack and flow battery (RED-FB) system capable of capturing, storing, and discharging salinity gradient energy. Energy captured from the RED stack was discharged in the flow battery at a maximum power density of 3.0 kW m^{-2}-anode, which was similar to the flow batteries charged by electrical power and could be used for practical applications. Salinity gradient energy captured from the RED stack was recovered from the electrolytes as electricity with 30% efficiency, and the maximum energy density of the system was 2.4 kWh m^{-3}-anolyte. The combined RED-FB system overcomes many limitations of previous approaches to capture, store, and use salinity gradient energy from natural or engineered sources.

Introduction

Salinity gradients naturally existing between river water and seawater could provide a large and renewable resource for clean energy production.[1] The global extractable energy from suitable river mouths is estimated to be 625 TWh per year, which is equivalent to 3% of the global electricity consumption.[2] Several salinity gradient energy (SGE) technologies have been proposed to capture this energy, including pressure-retarded osmosis (PRO),[3] reverse electrodialysis (RED),[4] capacitive mixing (CapMix),[5] and hydrogel expansion (HEx).[6] Among these SGE technologies, RED has the advantage of continuously converting energy into electricity.

A RED stack consists of an anode chamber, a series of membrane cells with alternating cation-exchange membranes (CEMs) and anion-exchange membranes (AEMs), and a cathode chamber.[7] If solutions with different salinities flow through channels separated by CEMs and AEMs, a voltage of approximately 0.1 to 0.2 V is generated across each membrane owing to the ion flux caused by the differences in salt concentrations.[1b,8] Cations are driven from high-concentration (HC) to low-concentration (LC) channels through CEMs, whereas anions are driven from HC to LC compartments through AEMs. A large number of pairs of CEMs and AEMs can be stacked together to increase the total voltage.[9] At both ends of the stack, electrodes are used to convert the ion flux into an electrical current through reduction–oxidation (i.e., redox) reactions at the electrodes, such as water splitting.[10] Reversible redox reactions (e.g., $[Fe(CN)_6]^{4-}$/$[Fe(CN)_6]^{3-}$ and Fe^{2+}/Fe^{3+}) that are recycled between the electrodes have been investigated to reduce the electrode overpotentials and, thus, to improve the power output.[10b] However, there has been no previous effort to extract energy from these redox couples. In addition, the power densities of RED stacks (typically ≈1 W m^{-2}-membrane) have been too low for practical applications.[1]

Recently, new types of organic redox-active energy carriers have been developed for use in flow batteries to increase their power and to avoid the need for rare and toxic metals such as vanadium and zinc.[11] For example, 2,6-dihydroxyanthraquinone (2,6-DHAQ, also referred to as DQ) and ferrocyanide ($[Fe(CN)_6^{4-}$, FC] redox couples used by Lin et al.[12] were composed entirely of earth-abundant elements that were nontoxic, nonflammable, and safe for use in residential and commercial environments. The main advantage of the flow battery is energy storage, as the liquid charged redox-active solutions can be stored in external tanks and then pumped into the cell for electricity generation when needed.[12,13] However, existing flow battery systems must be charged using electricity, and

[a] Dr. X. Zhu, Dr. T. Kim, Dr. C. A. Gorski, Dr. B. E. Logan
Department of Civil and Environmental Engineering
Penn State University
University Park, PA 16802 (USA)
Fax: (+1) 225-578-4945
E-mail: xzhu@lsu.edu

[b] Dr. X. Zhu
Department of Civil and Environmental Engineering
Louisiana State University
Baton Rouge, LA 70803 (USA)

[c] M. Rahimi
Department of Chemical Engineering
Penn State University
University Park, PA 16802 (USA)

Supporting Information for this article can be found under: http://dx.doi.org/10.1002/cssc.201601220.

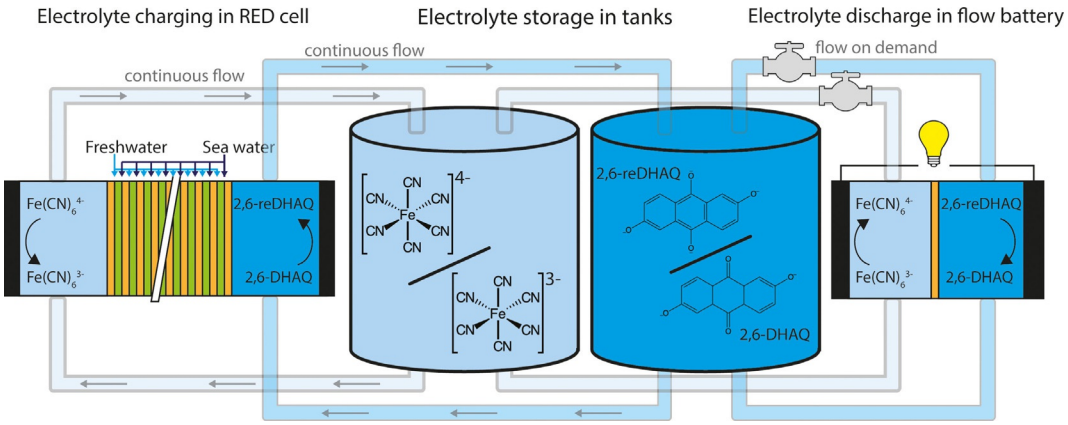

Figure 1. Schematic of the RED-FB system. RED: reverse electrodialysis; FB: flow battery.

they have not previously been used for conversion of other energy sources into electricity.

Herein, the electrolytes with FC-DQ redox couples were used in a RED stack to improve power extraction from natural salinity gradients and to provide energy storage. Unlike previous RED approaches for which the electrolytes were recycled, here the redox species were charged for energy storage. The energy in the redox couples was subsequently discharged in a flow battery to produce an integrated RED-flow battery (RED-FB) system to efficiently capture, store, and discharge salinity gradient energy (Figure 1 and Figure S1, Supporting Information). In the RED stack, the FC-DQ redox couples reduce the electrode overpotentials more than NaCl solution. During charging, $Fe(CN)_6^{4-}$ is oxidized to $Fe(CN)_6^{3-}$ at the anode and 2,6-DHAQ is reduced to 2,6-reDHAQ at the cathode. These two electrolyte solutions containing the charged redox couples are then pumped into the flow battery for discharging, in which $Fe(CN)_6^{3-}$ is reduced to $Fe(CN)_6^{4-}$ at the cathode and 2,6-reDHAQ is oxidized to 2,6-DHAQ at the anode. Thus, the RED stack recovers energy from salinity gradients, whereas the flow battery converts this energy into electrical power. Through the use of this integrated RED-FB system, salinity gradient energy is captured into solutions with a high energy density and is then discharged at much higher power densities in the flow battery than that possible by RED systems.

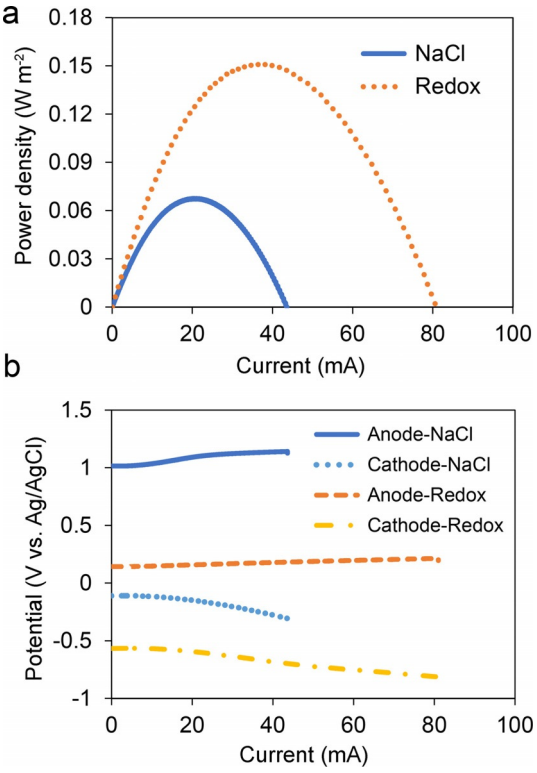

Figure 2. a) Power density normalized to the total active membrane area and b) electrode potentials of the RED stack with 0.6 M NaCl as the electrolyte or with the FC-DQ redox couple as the electrolyte.

Results and Discussion

Improved RED performance with redox couples

The power output of the RED stack was significantly improved relative to the power output of control tests with NaCl electrolytes upon using the FC-DQ redox couples as anolytes and catholytes (Figure 2a). The maximum power density increased from 0.07 $W m^{-2}$-membrane (2.8 $W m^{-2}$-anode) to 0.15 $W m^{-2}$-membrane (6.2 $W m^{-2}$-anode), the maximum current increased from 44 to 81 mA, and the energy recovery increased from 1.4 to 3.2%. The difference in power output was mainly due to the change in the electrode reactions. For control tests, oxygen evolution ($2H_2O \rightarrow O_2\uparrow + 4H^+$) occurred at the anode and hydrogen evolution ($2H_2O \rightarrow H_2\uparrow + 2OH^-$) took place at the cathode. For electrolytes with the two redox couples, $Fe(CN)_6^{4-}$ was oxidized at the anode and 2,6-DHAQ was reduced at the cathode. Because the electrode potentials of these reactions were different (Figure 2b), much less energy (0.7 V) was needed to drive the electrode reaction of the redox couples relative to that needed for oxygen and hydrogen evolution (1.2 V). Notably, higher power output and energy recovery could possibly be obtained by using the RED stack alone if reversible couples (e.g., $[Fe(CN)_6]^{4-}/[Fe(CN)_6]^{3-}$) were recycled between the electrodes to further reduce the electrode over-

potentials.[10b] However, electrolytes with two different redox couples (FC and DQ redox couples) were separately flowed through the electrodes chambers in the RED-FB system to capture and store the salinity gradient energy in the electrolytes.

Flow battery performance after RED charging at a salinity gradient of 100

The RED stack fed with NaCl solutions at a salinity gradient (SG) of 100 (HC: 0.6 M NaCl; LC: 0.006 M NaCl), representative of seawater (≈0.6 M) and river water (0.001–0.017 M),[14] was used to charge the FC-DQ redox couples for 4, 8, and 12 h (Figure 3a). The charging current was 30–40 mA, which produced total charging energies in the electrolyte couples of 352 (4 h), 705 (8 h), and 1058 J (12 h).

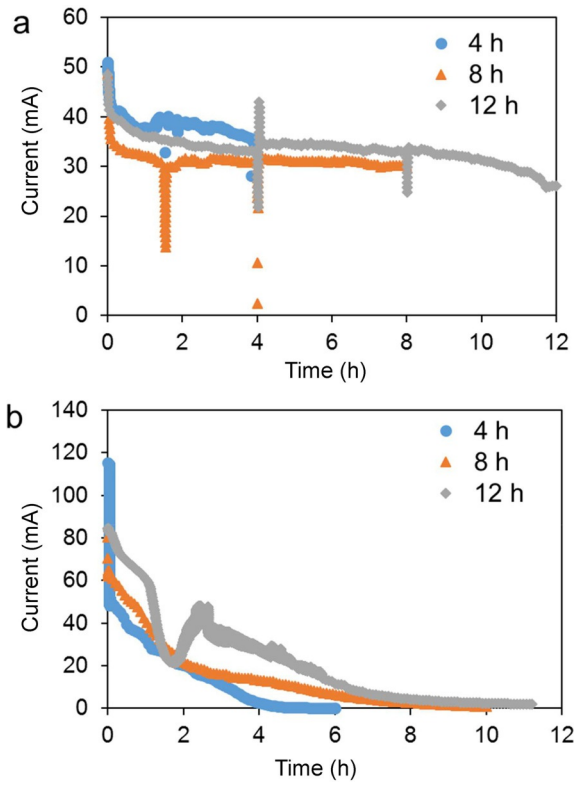

Figure 3. a) Charging current of the RED stack with the FC-DQ electrolytes; charging for 4, 8, and 12 h; and a salinity gradient of 100. The abrupt changes (shown by vertical lines) are due to replenishing of the HC and LC solutions. b) Discharging current of the flow battery with the three charged FC-DQ electrolytes. The reason for the abrupt drop and subsequent recovery may be due to temperature changes, because the test was run overnight.

The FC and DQ electrolytes were then cycled through the anode and cathode chambers of the flow battery to produce electricity. The discharge current at an external resistance of 10 Ω gradually decreased from approximately 50–80 mA to zero over a period of 4 h (4 h original charging time) or 8 h (8 and 12 h original charging time) (Figure 3b). The energies recovered from the discharging of the battery were 104 (4 h), 160 (8 h), and 349 J (12 h). On the basis of the volume of the

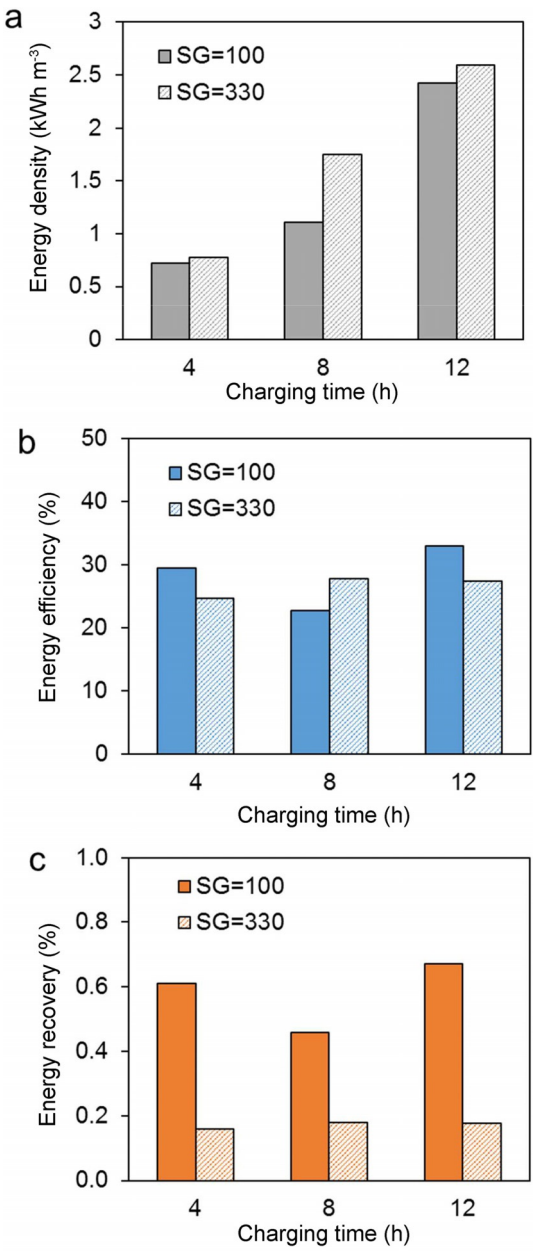

Figure 4. a) Energy density, b) energy efficiency, and c) energy recovery of the RED-FB system with the FC-DQ electrolytes; charging for 4, 8, and 12 h; and salinity gradients (SGs) of 100 and 330.

electrolyte (40 mL), the energy density ranged from 0.7 (4 h) to 2.4 kWh m^{-3} (12 h) (Figure 4a). The energy efficiencies, defined as the ratio between the discharging energy and the charging energy, were approximately 30% (Figure 4b). The energy recoveries based on the discharging energy and the input energy were approximately 0.55% (Figure 4c). The energy efficiency and recovery were relatively low. They could be improved by operating the RED stack at a maximum current without an external resistor and discharging the flow battery at maximum power with an external resistor similar to the internal resistance (≈3 Ω).

During the discharging tests that were used with a fixed resistance of 10 Ω, the average power densities were only 0.3

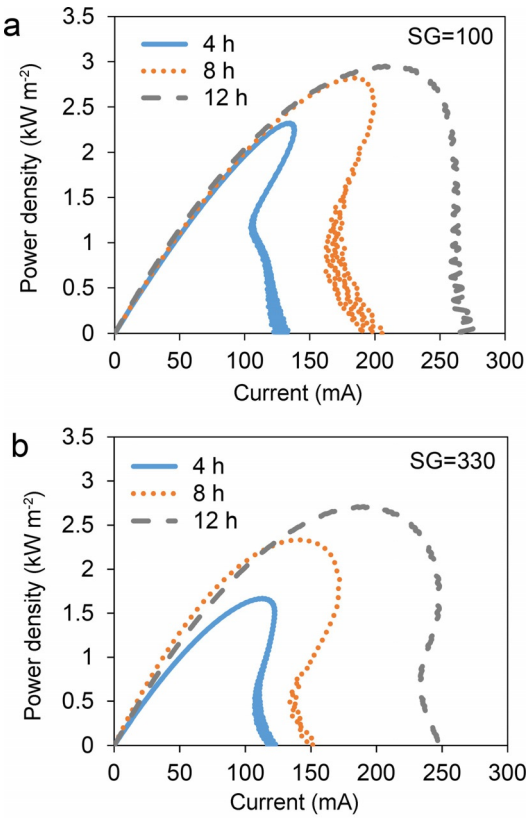

Figure 5. Power density of the RED-FB system during the discharge stage with the FC-DQ electrolytes; charging for 4, 8, and 12 h; and salinity ratios (SGs) of a) 100 and b) 330.

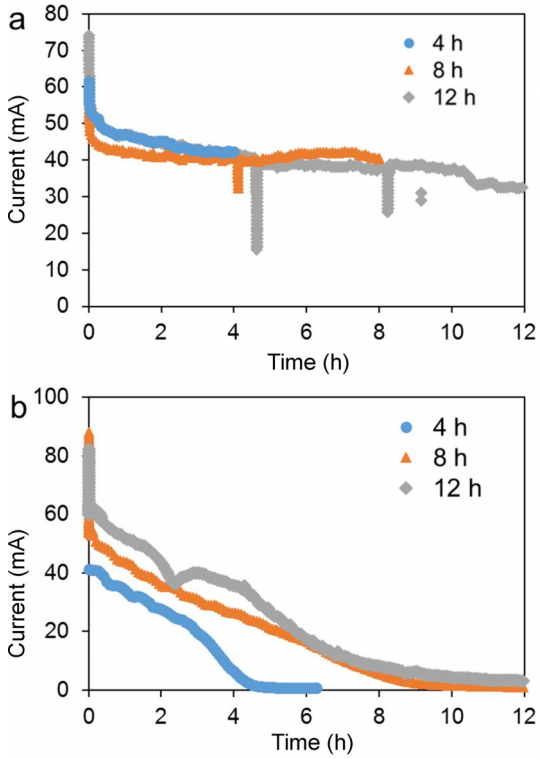

Figure 6. a) Charging current of the RED stack with the FC-DQ electrolytes; charging for 4, 8, and 12 h; and a salinity gradient of 330. The abrupt changes (shown by vertical lines) are due to replenishing of the HC and LC solutions. b) Discharging current of the flow battery with the three charged FC-DQ electrolytes.

(4 h), 0.4 (8 h), and 0.6 kW m^{-2}-anode (12 h). Polarization tests were conducted to obtain the maximum power density (Figure 5a), and they showed that the maximum power densities that could be extracted increased with the charging times, ranging from 2.4 (4 h) to 3.0 kW m^{-2}-anode (12 h).

Flow battery performance after RED charging at a salinity gradient of 330

The RED stack with feeding NaCl solutions at a large salinity gradient (SG) of 330 (HC: 2 M NaCl; LC: 0.006 M NaCl), representative of highly saline brine (0.6–6 M) and river water (0.001–0.017 M),[14] was also investigated to charge the FC-DQ redox couples for 4, 8, and 12 h (Figure 6a). The charging current (40–50 mA) was higher than that at a salinity gradient of 100 (≈30–40 mA), which resulted in larger charging energies in the electrolyte couples of 453 (4 h), 907 (8 h), and 1360 J (12 h).

Upon cycling the charged FC and DQ electrolytes through the anode and cathode chambers of the flow battery (fixed external resistance of 10 Ω), the current decreased from approximately 40–60 mA to zero over a longer period of 5 h (4 h original charging time) or 10 h (8 and 12 h original charging time) (Figure 6b). The energy recovered from discharging of the battery increased from 112 (4 h) to 373 J (12 h), and the energy density increased from 0.8 (4 h) to 2.6 kWh m^{-3} (12 h) (Figure 4a). The main advantage of the higher salinity gradient was faster charging with a reduced charging time to achieve the same energy density or a higher final energy density by using the same charging time. The energy efficiency was similar to that obtained by charging with the use of NaCl solutions at a salinity gradient of 100 (≈30%) (Figure 4b). However, the energy recovery (≈0.17%) was lower than that upon charging with the use of NaCl solutions at a salinity gradient of 100 (≈0.55%) (Figure 4c) probably as a result of more side reactions (e.g., water decomposition) and nonideal mass transport (e.g., undesirable ion and water transport through the ion-exchange membrane) with higher salinity solutions.[15] The energy efficiency and recovery could also be improved by operating the RED stack at maximum current without an external resistor and discharging the flow battery at maximum power with an external resistor similar to the internal resistance (≈3 Ω).

The average power densities during the discharge tests with a fixed resistance of 10 Ω were only 0.2 (4 h) and 0.4 kW m^{-2}-anode (12 h), whereas the maximum power densities obtained in the polarization tests ranged from 1.7 (4 h) to 2.7 W m^{-2}-anode (12 h) (Figure 5b). Relative to the power densities obtained by charging NaCl solutions at a salinity gradient of 100, these power densities were a little lower, mainly because of the absence of NaCl in the electrolytes (to avoid the precipitation of 2,6-DHAQ with Na^+), which resulted in lower electrolyte

conductivity and, therefore, more internal resistance (data for the NaCl experiments are reported in Figure S2).

RED-FB performance analysis

Previous approaches for extracting energy from salinity gradients have relied upon simultaneous energy extraction and electricity production.[4a,5a,16] In contrast, the RED-FB system developed here allows for energy storage, as the energy extracted from the salinity gradients is stored in the FC-DQ redox couple solutions, which can then be used for power generation when needed. The power densities were significantly improved upon using the flow battery for harvesting electrical power rather than directly in the RED stack. The maximum power density of the flow battery reached 3.0 kW m^{-2}-anode after charging by the RED stack for 12 h at a salinity gradient ratio of 100, which is similar to that of flow batteries charged by electrical power[11e,12] and can be used for practical applications. The energy density of the solutions used for power production was also greatly enhanced. The maximum theoretical energy density of the two NaCl solutions with equivalent volumes at a salinity gradient ratio of 100 (HC: 0.6 M NaCl; LC: 0.006 M NaCl) is 0.5 kWh m^{-3}-LC solution volume on the basis of Equation (6) (see the Experimental Section). Considering that the energy recovery of a RED stack is usually much less than 100% (e.g., 1.4% here without redox couples), the actual energy density of NaCl solutions in RED stacks would be approximately 7 Wh m^{-3}, which is only 0.3% of the actual energy density of the FC-DQ redox couple solutions produced for use in the flow battery of up to 2.4 kWh m^{-3} (RED stack charging for 12 h, salinity gradient ratio of 100). Thus, through charging the redox couples in the RED stack, the salinity gradient energy was efficiently stored at much greater densities in the redox solutions, which could subsequently be used as needed.

The energy efficiencies of the RED-FB system, which is the recovered electrical energy (discharging energy) relative to the charging energy, were approximately 30%. The loss of part of the energy resulted from several different processes. First, non-ideal mass transport (e.g., undesirable ion and water transport through the ion-exchange membrane) in the RED stack could result in partial energy loss. This could be reduced by using more selective membranes.[15] Second, side reactions (oxygen and hydrogen evolution) could have occurred at the anode and cathode of the RED stacks instead of charging redox couples. This energy loss could be better controlled by adjusting the salinity gradient, external resistances, and number of cell pairs in the RED stack. Third, part of the energy in the electrolytes with charged FC-HQ redox couples was remained in the RED stack and was not transferred into the flow battery for discharging. This loss should be negligible for greater amounts of electrolytes in larger scale systems. Fourth, oxygen could have leaked into the electrolytes through tubes and fittings, which would have directly oxidized 2,6-reDHAQ. This could be avoided with better designs that use less oxygen-permeable fittings and tubing. Fifth, Na^+ ions will be transported into the catholyte to balance the charge in the RED stack, which could result in precipitation of 2,6-DHAQ if the Na^+ concentration becomes too high. This might be resolved by using other catholytes (such as Br_2[11d] and methyl viologen)[11a,b] instead of 2,6-DHAQ or by limiting energy storage with a low concentration of 2,6-DHAQ. Alternatively, ammonium bicarbonate rather than NaCl solutions could be used in the RED stack for waste heat energy recovery.[15b,17]

The energy recoveries of the RED-FB system, which is the ratio between total recovered electrical energy and total energy input into the system, were approximately 0.55 (SG = 100) and 0.17% (SG = 330). This extent of energy recovery is relatively low, but it could easily be increased by improving the configuration and operation conditions, as the RED stack conditions used here were not optimized. For example, previous studies demonstrated that RED energy production could be improved by using profiled membranes to reduce internal resistance[18] and the efficiency of energy extraction could be optimized by adjusting the HC and LC flow rates.[4b,7b] With equal volumes of seawater and river water, the energy recovery of the RED stacks could reach approximately 83%.[4a,19] Therefore, the energy recovery of the RED-FB system could be improved to 25% even with an energy efficiency of 30%.

Other applications

Thermolytic salts that can be distilled from water at relatively low temperatures, such as ammonium bicarbonate (AmB), can be used to create synthetic salinity gradients by waste heat, and as much as approximately 1 TW is estimated to be available from industries in the USA alone.[17b,20] With AmB, the maximum power of a RED system is approximately 6.3 W m^{-2}-anode ($\approx$0.3 W m^{-2}-membrane) and the energy recovery is approximately 2–6%.[15b,17a] Thus, the RED-FB system could also be used as a method for energy extraction, storage, and generation from waste heat by using AmB.[15b,17] In addition, other redox couples with higher energy densities and lower electrode overpotentials could be developed for use in the RED-FB, and they might further improve the energy recovery relative to that of the FC-DQ redox couples tested here.

Conclusions

Through integrating a reverse electrodialysis stack with a flow battery (RED-FB system), salinity gradient energy was harvested in a flow battery with a maximum power density of 3.0 kW m^{-2}-anode, which was much higher than that of a RED stack alone (0.07 W m^{-2}-membrane or 2.8 W m^{-2}-anode). The energy density was also increased from 7 (RED with NaCl solutions) to 2.4 kWh m^{-3} (flow battery with redox couple solutions). This combined energy extraction and generation approach could make the recovery of salinity gradient energy more practical. The salinity gradient energy can be first stored in solutions with redox couples at an energy density much higher than NaCl solutions through a RED stack. Later, it can be used for extensive applications with a high power density when it is needed.

Experimental Section

RED-BF system construction and operation

The RED stack was constructed by using a commercially available 20-cell-pair electrodialysis stack (PCCell GmbH, ED 64002-020, Heusweiler, Germany) as shown in Figure S1.[4b,15b] Both electrodes were titanium mesh coated with platinum and iridium (Ti/Pt-Ir), with a projected area of 64 cm^2 (8 cm × 8 cm). Ag/AgCl reference electrodes (210 mV vs. a standard hydrogen electrode, SHE) were inserted into the anode and cathode chambers to record the anode and cathode potentials. The membrane stack was assembled with 21 standard CEMs (PC-SK) and 20 standard AEMs (PC-SA) supplied by the manufacturer, each with an active membrane area of 64 cm^2 (8 cm × 8 cm), for a total active membrane area of 0.26 m^2. The thickness of spacers between the membranes was 0.5 mm. High concentration (HC; 0.6 M NaCl or 2 M NaCl) and low concentration (LC; 0.006 M NaCl) solutions were separately pumped through the HC and LC channels of the stack in a single-pass mode at flow rates of 40 mL min^{-1}. The anolyte and catholyte (each 40 mL) were purged with ultrahigh purity argon to ensure deaeration before all tests and were then recycled through the anode and cathode chambers at flow rates of 100 mL min^{-1}. For control tests (RED alone) without redox couples, both the anolyte and catholyte were 0.6 M NaCl. For RED-FB tests with redox couples and a salinity ratio of 100 (HC: 0.6 M NaCl; LC: 0.006 M NaCl), the anolyte was 0.4 M $K_4Fe(CN)_6$, 1 M KOH, and 0.6 M NaCl and the catholyte was 0.2 M 2,6-DHAQ, 1 M KOH, and 0.6 M NaCl. For RED-FB tests with redox couples and a salinity ratio of 330 (HC: 2 M NaCl; LC: 0.006 M NaCl), the anolyte was 0.4 M $K_4Fe(CN)_6$ and 1 M KOH and the catholyte was 0.2 M 2,6-DHAQ and 1 M KOH, without 0.6 M NaCl to avoid precipitation resulting from the greater amount of Na^+ ion transport into the electrolytes that resulted from the increased current and the use of the higher salinity solutions. KOH (1 M) was added in both cases to increase the solubility of 2,6-DHAQ, as it has higher solubility in more alkaline solutions.

The flow battery was constructed by using commercial hardware (Se-Nr 090820010, H-TEC) as shown in Figure S1. Two pieces of porous carbon paper (2050-1550, Clean Fuel Cell Energy, LLC) with a size of 4 cm × 5 mm were used as the anode and cathode, and they were pretreated by immersing in a 1:3 *v/v* mixture of concentrated nitric acid and sulfuric acid overnight and then rinsing with deionized water. The two electrodes were pressed onto opposite sides of a cation-exchange membrane (Selemion CMV). Then, two thin Ti plates with 16 2 mm-diameter holes were separately pressed onto the back of carbon paper electrodes as current collectors, which resulted in a working surface area of 0.5 cm^2 for carbon paper electrodes. Between the two Ti current collectors and end-plates, the anode and cathode chambers were formed by two gaskets with a thickness of approximately 2 mm. Then, the whole cell was clamped together by using screw rods and nuts. The solutions with charged redox couples by RED were recycled through the anode and cathode chambers of the flow battery at a flow rate of 100 mL min^{-1} for discharging tests.

Performance tests

Polarization tests were performed to obtain the power density of the RED stack and the flow battery by using a potentiostat (Bio-Logic, VMP3). Cell voltages were decreased from the open-circuit voltage (OCV) to 0 V versus the cathode potential (short circuit) at a scan rate of 100 mV s^{-1}. Currents were recorded by using EC-Lab V10.02 software. The power density (P) of the RED stack or flow battery was calculated by using Equation (1):

$$P = \frac{UI}{A} \quad (1)$$

in which U is the cell voltage, I is the measured current, and A is the total active membrane area (0.26 m^2) for the RED stack, and the projected anode or cathode surface area for the flow battery (each 0.5 cm^2).

During charging of the redox solutions in the RED system, if no external resistor was used, the system could be operated at the maximum current, with all the recovered energy used to charge the redox solutions. However, to measure the charging current during the tests ($I_c = U_R/R$), an external resistor (R) of 10 Ω was added between the anode and the cathode of the RED stack, with the voltage (U_R) over the resistor recorded. Therefore, part of the energy was dissipated through the external resistor, which is defined here as energy lost to the resistor (E_R), determined by Equation (2):

$$E_R = \int_0^{t_c} U_R I_c \mathrm{d}t \quad (2)$$

in which U_R is the cell voltage (i.e., the voltage over the resistor), I_c is the charging current, and t_c is the charging time. The energy that was used to charge the redox solutions, called the charging energy (E_c), was calculated by using Equation (3):

$$E_c = \int_0^{t_c} U_c I_c \mathrm{d}t \quad (3)$$

in which U_c is the charging voltage (i.e., the difference of electrode potentials, ≈ 0.7 V for FC-DQ redox couples), I_c is the charging current, and t_c is the charging time.

After charging in the RED stack, the anolyte and catholyte were purged with ultrahigh purity argon again and pumped into the flow battery for discharging tests. During the discharging processes, the anode and cathode of the flow battery were connected with an external resistor (R) of 10 Ω to obtain the cell voltage (U_d). The discharging current was obtained by using Equation (4), and the discharging energy (E_d) (recovered energy) was calculated from Equation (5):

$$I_d = \frac{U_d}{R} \quad (4)$$

$$E_d = \int_0^{t_d} U_d I_d \mathrm{d}t \quad (5)$$

in which U_d is the discharging cell voltage, I_d is the discharging current, and t_d is the discharging time. Notably, the FB was discharged by using an external resistor of 10 Ω, rather than by using a smaller resistor (≈3 Ω) at which the maximum power could be produced to obtain a stable power output.

Energy calculations

The total energy input to the system (E^{in}) was estimated by the change in the free energy for the complete mixing of the HC and LC solutions according to Equation (6):

$$E^{in} = RT\sum_{i}(V_{HC}c^{in}_{i,HC}\ln\frac{a^{in}_{i,HC}}{a_{i,M}} + V_{LC}c^{in}_{i,LC}\ln\frac{a^{in}_{i,LC}}{a_{i,M}}) \quad (6)$$

in which R (8.314 J mol^{-1} K^{-1}) is the gas constant, T (298 K) is the absolute temperature, V (L) is the volume of solutions, c (mol L^{-1}) is the molar concentration of ionic species i in the solution, and a is the activity of ionic species i in the solution. The subscripts denote high-concentration (HC), low-concentration (LC), and mixed (M) solutions. The energy densities of the NaCl solutions were calculated by normalizing E^{in} to the equivalent volume of the HC or LC solution (1 m^3 each). The energy density of solutions with redox couples was obtained by normalizing recovered energy (discharging energy) to the volume of anolyte or catholyte (each 40 mL). The energy efficiency was defined as the ratio between recovered energy (discharging energy) and charging energy. The energy recovery of the RED stack alone was calculated on the basis of the maximum power output of the RED stack obtained by the polarization test and the energy input per second obtained according to Equation (6). The energy recovery of the RED-FB system was determined as the recovered energy (discharging energy) over the total energy input to the system (E^{in}).

Acknowledgements

This research was supported by the National Science Foundation (NSF) through the award of CBET-1464891.

Keywords: energy conversion · flow batteries · reverse electrodialysis · salinity gradient · sustainable chemistry

[1] a) B. E. Logan, M. Elimelech, *Nature* **2012**, *488*, 313 – 319; b) G. Z. Ramon, B. J. Feinberg, E. M. V. Hoek, *Energy Environ. Sci.* **2011**, *4*, 4423 – 4434.
[2] a) G. L. Wick, W. R. Schmitt, *Mar. Technol. Soc. J.* **1977**, *11*, 16 – 21; b) J. D. Isaacs, R. J. Seymour, *Int. J. Environ. Stud.* **1973**, *4*, 201 – 205; c) O. A. Alvarez-Silva, A. F. Osorio, C. Winter, *Renewable Sustainable Energy Rev.* **2016**, *60*, 1387 – 1395.
[3] A. Achilli, A. E. Childress, *Desalination* **2010**, *261*, 205 – 211.
[4] a) J. W. Post, H. V. M. Hamelers, C. J. N. Buisman, *Environ. Sci. Technol.* **2008**, *42*, 5785 – 5790; b) X. P. Zhu, W. H. He, B. E. Logan, *J. Membr. Sci.* **2015**, *486*, 215 – 221.
[5] a) D. Brogioli, *Phys. Rev. Lett.* **2009**, *103*, 058501; b) M. C. Hatzell, K. B. Hatzell, B. E. Logan, *Environ. Sci. Technol. Lett.* **2014**, *1*, 474 – 478.
[6] X. P. Zhu, W. L. Yang, M. C. Hatzell, B. E. Logan, *Environ. Sci. Technol.* **2014**, *48*, 7157 – 7163.
[7] a) E. Güler, R. Elizen, D. A. Vermaas, M. Saakes, K. Nijmeijer, *J. Membr. Sci.* **2013**, *446*, 266 – 276; b) J. Veerman, M. Saakes, S. J. Metz, G. J. Harmsen, *Environ. Sci. Technol.* **2010**, *44*, 9207 – 9212.
[8] D. A. Vermaas, E. Guler, M. Saakes, K. Nijmeijer, *Energy Procedia* **2012**, *20*, 170 – 184.
[9] J. Veerman, M. Saakes, S. J. Metz, G. J. Harmsen, *J. Membr. Sci.* **2009**, *327*, 136 – 144.
[10] a) P. Długołecki, A. Gambier, K. Nijmeijer, M. Wessling, *Environ. Sci. Technol.* **2009**, *43*, 6888 – 6894; b) J. Veerman, M. Saakes, S. J. Metz, G. J. Harmsen, *J. Appl. Electrochem.* **2010**, *40*, 1461 – 1474.
[11] a) T. Janoschka, N. Martin, U. Martin, C. Friebe, S. Morgenstern, H. Hiller, M. D. Hager, U. S. Schubert, *Nature* **2015**, *527*, 78 – 81; b) T. B. Liu, X. L. Wei, Z. M. Nie, V. Sprenkle, W. Wang, *Adv. Energy Mater.* **2016**, *6*, 1501449; c) Q. Chen, L. Eisenach, M. J. Aziz, *J. Electrochem. Soc.* **2016**, *163*, A5057 – A5063; d) B. Huskinson, M. P. Marshak, C. Suh, S. Er, M. R. Gerhardt, C. J. Galvin, X. D. Chen, A. Aspuru-Guzik, R. G. Gordon, M. J. Aziz, *Nature* **2014**, *505*, 195 – 198; e) Q. Chen, M. R. Gerhardt, L. Hartle, M. J. Aziz, *J. Electrochem. Soc.* **2016**, *163*, A5010 – A5013.
[12] K. X. Lin, Q. Chen, M. R. Gerhardt, L. C. Tong, S. B. Kim, L. Eisenach, A. W. Valle, D. Hardee, R. G. Gordon, M. J. Aziz, M. P. Marshak, *Science* **2015**, *349*, 1529 – 1532.
[13] G. L. Soloveichik, *Chem. Rev.* **2015**, *115*, 11533 – 11558.
[14] A. F. Pillsbury, *Sci. Am.* **1981**, *245*, 54.
[15] a) A. Daniilidis, D. A. Vermaas, R. Herber, K. Nijmeijer, *Renewable Energy* **2014**, *64*, 123 – 131; b) X. P. Zhu, W. H. He, B. E. Logan, *J. Membr. Sci.* **2015**, *494*, 154 – 160.
[16] F. La Mantia, M. Pasta, H. D. Deshazer, B. E. Logan, Y. Cui, *Nano Lett.* **2011**, *11*, 1810 – 1813.
[17] a) M. C. Hatzell, I. Ivanov, R. D. Cusick, X. P. Zhu, B. E. Logan, *Phys. Chem. Chem. Phys.* **2014**, *16*, 1632 – 1638; b) R. D. Cusick, Y. Kim, B. E. Logan, *Science* **2012**, *335*, 1474 – 1477.
[18] a) D. A. Vermaas, M. Saakes, K. Nijmeijer, *J. Membr. Sci.* **2011**, *385*, 234 – 242; b) D. A. Vermaas, M. Saakes, K. Nijmeijer, *J. Membr. Sci.* **2014**, *453*, 312 – 319.
[19] N. Y. Yip, D. A. Vermaas, K. Nijmeijer, M. Elimelech, *Environ. Sci. Technol.* **2014**, *48*, 4925 – 4936.
[20] a) A. P. Straub, N. Y. Yip, S. Lin, J. Lee, M. Elimelech, *Nat. Energy* **2016**, *1*, 16090; b) X. P. Zhu, M. Rahimi, C. A. Gorski, B. Logan, *ChemSusChem* **2016**, *9*, 873 – 879.

Manuscript received: September 1, 2016
Revised: November 29, 2016
Accepted Article published: December 1, 2016
Final Article published: January 25, 2017